PHYSICAL REVIEW C **80**, 021304(R) (2009)

Di-neutron correlations in ^{7}H

S. Aoyama[1] and N. Itagaki[2]
[1]*Integrated Information Processing Center, Niigata University, Niigata 950-2181, Japan*
[2]*Department of Physics, University of Tokyo, Hongo, Tokyo 113-0033, Japan*
(Received 18 January 2009; revised manuscript received 20 July 2009; published 19 August 2009)

We investigate the dineutron correlations in ^{7}H. The ground state of ^{7}H is solved by superposing many AMD (antisymmetrized molecular dynamics) Slater determinants with various $t+n+n+n+n$ configurations based on AMD triple-S (AMD superposition of selected snapshots). The mixing of dineutron cluster components is estimated by calculating the squared overlap with the wave function of the dineutron condensate, which is an extension of the studies on the α condensate in $4N$ nuclei. The calculated results show significant mixing of components of dineutron clusters ($t+{}^{2}n+{}^{2}n$) with a spatially extended distribution ($\sim$70%) much larger than that of ^{8}He, where the core nucleus is changed from t to ^{4}He.

DOI: 10.1103/PhysRevC.80.021304 PACS number(s): 21.10.Gv, 21.60.Gx, 27.10.+h, 27.20.+n

The studies of neutron-rich nuclei have attracted much interest because they have been continually giving us new knowledge of extreme nuclei. Among them, it is a challenging subject to study nuclei with maximal ratios of neutron to proton numbers, which give fundamental information for the nature of nuclear force and nuclear matter in extreme conditions. It is ^{7}H that has the maximal ratio ($N/Z=6$) observed so far, and the value even reaches the one for the surface of the neutron star. Quite recently, ^{7}H was observed with a peak structure above the $t+n+n+n+n$ threshold energy in the proton transfer experiment by Caamaño *et al.* at GANIL [1,2]. The resonance energy was derived as $E=0.57$ MeV from the $t+n+n+n+n$ threshold although the number of events was very limited. This experiment confirms the first evidence of ^{7}H shown by Korsheninnikov *et al.* in the $p(^{8}\text{He},pp)^{7}$H reaction at RIKEN [3].

In such weakly bound systems, the dineutron (neutron-neutron) correlation becomes extremely important as discussed by many authors (see Refs. [4–7] and references therein). For example, for the ground state of ^{6}He, the $^{4}\text{He}+n+n$ three-body model calculations show the coexistence of the dineutron (boson) and the two neutrons (fermions) in the p-shell around the ^{4}He core [7]. Recently, this coexistent nature of the two neutron states has been reinterpreted in association with the BCS-BEC crossover phenomenon [8,9]. As for the two dineutron case, a candidate is ^{8}He ($^{4}\text{He}+{}^{2}n+{}^{2}n$). Here, the separation energy of neutrons is small as in the case of ^{6}He and the neutrons have a spatially extended distribution. Therefore, it is considered that the formation of the dineutrons is favored and the $^{4}\text{He}+{}^{2}n+{}^{2}n$ (two bosons around the core) components mix significantly to the $^{4}\text{He}+n+n+n+n$ (four fermions around the core) configurations.

Such boson-like correlations in dilute systems have been also studied in $4N$ nuclei with α-cluster structures [10], e.g., the second 0^{+} state of ^{12}C. Tohsaki *et al.* [10] suggest that in light $4N$ nuclei some of the excited states are interpreted as boson condensates comprising several α's. It is rather surprising that the second 0^{+} state of ^{12}C is dominantly described by a simple condensed-type wave function ($\sim$90%), which is called the THRS (Tohsaki-Horiuchi-Schuck-Röpke) wave function [11]. To extend the discussion to the dineutron condensate along the lines of such studies, we have studied ^{8}He by introducing the THRS wave function around the ^{4}He core [12]. The calculated results show the coexistence of dineutrons and shell-model-like structures [12,13].

It is considered that in small neutron density regions, such a Boson-like (dineutron) cluster correlation becomes strong. However, because there is no external field for ^{8}He or ^{6}He to control the neutron density, one possible way to prove this hypothesis is to pick up one proton from the ^{4}He core. This makes the core-n interaction weaker. Therefore, here we perform the study on H isotopes from such a view point. There are some pioneering works for ^{7}H [14,15] but detailed discussions have not been fully given mainly due to the large computational time. For example, in our previous work [14], we did not have enough computational power to get the converged solution. Also, in the work by Timofeyuk [15], the final result is not obtained, and she has made a prediction for the low-lying state by a kind of extrapolation method. Here the method and the interaction are slightly different from ours. Although He isotopes have been studied by many authors, the studies on H isotopes are quite few. Both isotopes might have similarities, but they would also have differences originating from the weaker core-n interaction and the spin nonsaturated effect of the triton core in ^{7}H. Thus, the simultaneous understanding of both isotopes is desirable. Now the new experimental results are given [1] and we have a new theoretical framework and enough computational power [12,16]; thus it is the time to analyze ^{7}H again. Here, the new concept of a dineutron condensate [8,9] is introduced to ^{7}H.

In this study, we solve the five-body problems by using the so-called antisymmetrized molecular dynamics (AMD) triple-S (superposition of selected snapshots) and give an analysis of the dineutron correlations in ^{7}H for the first time. We show the development of the clusterization of dineutrons from ^{8}He to ^{7}H by calculating the overlap between the solutions of five-body models and the THSR-type wave function. We also compare the results of the similar analyses of ^{6}He and ^{5}H.

We briefly describe the present method which is called the AMD triple-S [17]. The wave function of the present framework is given as

$$\Psi^{JM\pi} = \sum_i c_i P^J_{MK} P^\pi \Phi_k, \quad (1)$$

where $i = \{k, K\}$. Here, $\{\Phi_k\}$ are Slater determinants (i.e., conventional AMD wave functions) explained below, and they are projected onto a good angular momentum (parity) by the projection operator P^J_{MK} (P^π). The coefficients c_i are determined by diagonalizing the Hamiltonian matrix after these projections; thus $\{\Phi_k\}$ are regarded as basis functions. We select the important basis functions based on the technique of the stochastic variational method (SVM) [17–19]: we employ only the basis functions with which we get sufficient binding-energy gain.

Each basis function, Φ_k, is fully antisymmetrized by the operator $\mathcal{A}$,

$$\Phi_k = \mathcal{A}[(\psi_1\chi_1)(\psi_2\chi_2)\cdots(\psi_A\chi_A)]_k, \quad (2)$$

and $\psi_i\chi_i$ corresponds to the wave function of each nucleon (ψ, spatial part; χ_i, spin-isospin part), and ψ_i is represented by a Gaussian form,

$$\psi_i = \left(\frac{2\nu}{\pi}\right)^{\frac{3}{4}} \exp\left[-\nu\left(\boldsymbol{r} - \frac{\boldsymbol{Z}_i}{\sqrt{\nu}}\right)^2\right], \quad (3)$$

where $\boldsymbol{Z}_i$ is a Gaussian center parameter with a complex value. The real and imaginary parts of $\frac{\mathbf{Z}_i}{\sqrt{\nu}}$ are associated with the position and the momentum of the single particle. The oscillator parameter ($b = \frac{1}{\sqrt{2\nu}}$) is common for all the nucleons to exactly remove the center-of-mass kinetic energy. We assume the presence of a triton (t) cluster by giving a common $\boldsymbol{Z}_i$ value for the three nucleons (one proton and two neutrons). In each basis function Φ_k, the values of $\boldsymbol{Z}_i$ for valence neutrons are randomly generated and we optimize their imaginary parts by using the frictional cooling method of the AMD [17].

To estimate the mixing of dineutron condensate in ^{7}H, we calculate the squared overlap between the AMD triple-S wave function and the THSR wave function [12,13]. The THSR wave function was originally proposed for the α condensate such as the second 0^+ state of ^{12}C [10,20], and the extension of the THSR wave function to describe the dineutron-like states in ^{8}He has been carried out [12,13].

In a similar way, the THSR-type wave function is introduced for ^{7}H, which describes the motion of two dineutron clusters, $\Phi^\sigma_1(2n)$ and $\Phi^\sigma_2(2n)$, around the triton core, $\Phi(t)$:

$$\Phi^\sigma_{\rm THSR}(^7{\rm H}) = \mathcal{A}\big[\Phi(t)\Phi^\sigma_1(2n)\Phi^\sigma_2(2n)\big], \quad (4)$$

$$\Phi(t) = G_t(\boldsymbol{R}_0)\chi^{p\uparrow n\uparrow n\downarrow}, \quad (5)$$

$$\Phi^\sigma_{\rm k}(2n) = \int d\boldsymbol{R}_k G_{2n}(\boldsymbol{R}_{\rm k}) \exp\left(-\frac{\boldsymbol{R}_k^2}{\sigma^2}\right)\chi^{n\uparrow n\downarrow}. \quad (6)$$

Here, the nucleons in the same cluster have the common spatial part of the wave function with the Gaussian form centered at $\boldsymbol{R}_i$ $(i = 0, 1, 2)$, $G_{(t,2n)}(\boldsymbol{R}_i) \propto \Pi_\alpha \exp(-\nu(\boldsymbol{r}_\alpha - \boldsymbol{R}_i)^2)$, where $G_t(\boldsymbol{R}_0)$ and $G_{2n}(\boldsymbol{R}_k)$ $(k = 1, 2)$ are for the triton and dineutron clusters and α denotes the nucleons inside each cluster. Also, $\chi^{p\uparrow n\uparrow n\downarrow}$ and $\chi^{n\uparrow n\downarrow}$ are the spin-isospin parts of the triton and dineutron clusters.

In the present study, we replace the integration for $\boldsymbol{R}_k$ with the summation of the many Slater determinants [21],

$$\Phi^\sigma_{\rm THSR}(^7{\rm H}) = \sum_{I=1}^{I_{\rm max}} \Phi^{I,\sigma}_{\rm Mont}(^7{\rm H}), \quad (7)$$

$$\Phi^{I,\sigma}_{\rm Mont}(^7{\rm H}) = \mathcal{A}\big[G_t(\boldsymbol{R}_0)G_{2n}\big(\boldsymbol{R}^I_1\big)G_{2n}(\boldsymbol{R}^I_2)\chi\big], \quad (8)$$

where I's are a set of the Gaussian center parameters $\boldsymbol{R}_k$ $(k = 1, 2)$ for the dineutron clusters and χ is the spin and isospin parts of the total system. The parameters $\boldsymbol{R}^I_k(I = 1, 2, \ldots, I_{\rm max})$ are generated by the weight function W with a Gaussian shape [21]. With increasing the ensemble number ($I_{\rm max}$), the distribution approaches the Gaussian with a width parameter of σ. Thus, it is considered that the integration over the Gaussian center parameters in the original THSR wave function is expressed as the superposition of the AMD Slater determinants (i.e., Monte Carlo integration). To reduce the number of basis functions ($I_{\rm max}$), we numerically project out the total angler momentum of the system. The angular momentum is projected to $1/2^+$, because the intrinsic spin of the triton and dineutron clusters are $1/2^+$ and 0^+, respectively, and each dineutron is in the S orbit around the triton:

$$\Psi^{JM\pi,\sigma}_{\rm THSR}(^7{\rm H}) = \sum_K P^\pi P^J_{MK}\Phi^\sigma_{\rm THSR}(^7{\rm H}), \quad (9)$$

where P^π and P^J_{MK} are the projection operator for the parity and the angler momentum, respectively (in the present study, π is + and $J = M = K = \frac{1}{2}$).

The Hamiltonian operator ($\hat{H}$) has the following form:

$$\hat{H} = \sum_{i=1}^A \hat{t}_i - \hat{T}_{\rm c.m.} + \sum_{i>j}^A \hat{v}_{ij}, \quad (10)$$

where the two-body interaction ($\hat{v}_{ij}$) includes the central part, the spin-orbit part, and the Coulomb part. For the central part, the Volkov No. 2 potential is employed [22]:

$$V_{\rm cnt}(r) = (W - MP^\sigma P^\tau + BP^\sigma - HP^\tau) \times \big[V_1\exp\big(-r^2/c_1^2\big) + V_2\exp\big(-r^2/c_2^2\big)\big]. \quad (11)$$

The original Volkov No. 2 potential ($W = 1 - M, M = 0.60, B = H = 0$) gives a bound state for the n-n system, but it is eliminated by introducing B and H parameters. In this article, we use $B = H = 0.07$, which reproduces the barely unbound property of the dineutron system ($E_{\rm cal} = 0.05$ MeV) within the present model space (However B and H should be ∼0.1 to get this value in the full model space). Also, $M = 0.56$ ($E = 1.0$ MeV) is determined to be consistent with the experimental ground state energy ($E_{\rm exp.} = 1.7$ MeV) [23] for ^{5}H. For the spin-orbit term, the G3RS potential [24] is employed as

$$V_{ls}(r) = V_0\big\{e^{-d_1r^2} - e^{-d_2r^2}\big\}P(^3{\rm O})\vec{L}\cdot\vec{S}, \quad (12)$$

where $d_1 = 5.0$ fm^{-2}, $d_2 = 2.778$ fm^{-2}, $V_0 = 2000$ MeV [25], and $P(^3{\rm O})$ is a projection operator onto a triplet odd state.

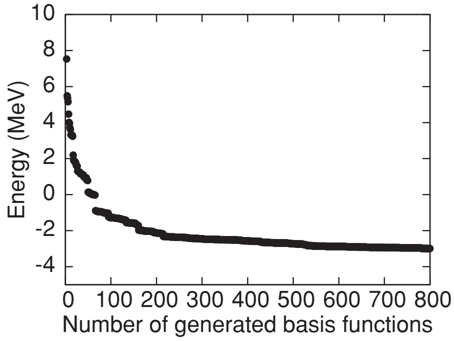

FIG. 1. The energy convergence of the ground state ($1/2^+$) of ^{7}H based on the generator coordinate method (GCM). The energy is obtained by diagonalizing the Hamiltonian and plotted as a function of the number of generated basis functions (Slater determinants).

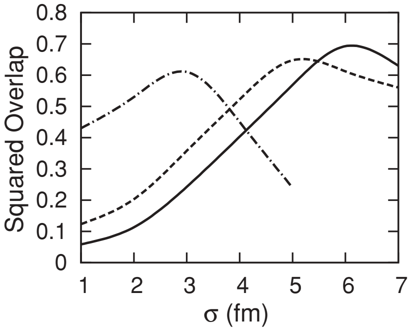

FIG. 2. The squared overlap between the obtained ground state and the THSR wave function: $|\langle\Psi^{1/2+}|\Psi^{1/2+\sigma}_{\rm THSR}\rangle|^2$. The solid (dotted) line corresponds to the squared overlap for ^{7}H with $M = 0.56$ ($M = 0.5$) and $B = H = 0.07$. The values (dash-dotted line) for ^{8}He are taken from Ref. [12]. The horizontal axis represents σ.

The operator $\vec{L}$ stands for the relative angular momentum and $\vec{S}$ is the spin ($\vec{S}_1 + \vec{S}_2$).

In Fig. 1, the energy convergence of the ground state ($1/2^+$) of ^{7}H is shown. The energy is obtained by diagonalizing the Hamiltonian and plotted as a function of the number of basis functions (the number of trial basis functions is 800). Here, we use a technique of SVM [19]: if a trial basis function contributes enough to the energy decrease after the diagonalization of the Hamiltonian, we employ it as a basis function. The selecting condition as a basis function is $\Delta E_3 = 0.01$ MeV [17], which means the decrease of the energy sum of the three lowest $1/2^+$ states by more than 10 keV. The converged energy is $E = -2.8$ MeV. Here, the oscillator parameter ($b = 1.71$ fm) is also chosen to give the minimum energy. Because the triton is calculated as -7.0 MeV within this model ($b = 1.71$ fm), the obtained state is 4.2 MeV above the $t + 4n$ threshold. To check the convergence, we carried out the calculation several times with different sets of basis functions; however, the difference in energy is of the order of 0.01 MeV. In this calculation, we only generated the basis functions with same number of spin-up and spin-down neutrons, $S_z = 0$. This is because $S = 1$ components for the valence neutrons could be already taken into account within the $S_z = 0$ basis states due to the rotational symmetry of the t core. To check it, we add 400 trial basis functions with $S_z = -1$ for the neutrons. Although we have tried several basis sets, the energy gain is always around the order of the energy convergence ($0.01 \sim 0.02$ MeV.)

In Fig. 2, the squared overlap between the obtained ground state and the THSR wave function is shown. The solid and dash-dotted lines correspond to the squared overlap for ^{7}H and ^{8}He [12], respectively. For each dineutron cluster, we do not solve the relative motion between two neutrons, and they are assumed to have a locally peaked $(0s_{1/2})^2$ configuration. In the THSR picture, the distribution of the Gaussian center parameters of these two dineutron clusters is described as the same spatially extended S orbit around the core. For ^{7}H, we can see a clear peak around $\sigma = 6$ fm at which the squared overlap is 0.69 (solid line). This large overlap (∼70%) at $\sigma = 6$ fm means that the major part of the ^{7}H structure is interpreted as two dineutrons in the same (extended) S orbit or, in other words, as the dineutron condensate. It is rather surprising that the ground state has such a large overlap: although the ground state calculated with the $t + n + n + n + n$ model is expected to have a shell-model-like structure with many complex configurations, the actual state has a simple t plus two dineutrons structure, which is mainly described by a THSR wave function. In this article, we employ $I_{\rm max} = 200$ in Eq. (7). This gives a numerical error of several percent for large σ values and of $\lesssim$1% for $\sigma = 1$ fm. Therefore, the above discussion would not be changed by the numerical uncertainty from the Monte Carlo integration. It is important to mention that other discretized continuum states of ^{7}H have almost zero overlap with the THSR wave function. Therefore, we can easily distinguish the present state from other continuum solutions.

It is worthwhile to compare the present results for ^{7}H with the results of ^{8}He in our previous article [12]. Here, we introduce a similar five-body model of ^{4}He + $n + n + n + n$. For ^{8}He, the skin (or halo) structure of four neutrons can be discussed in relation to the dineutron correlation (e.g., Ref. [26] and references therein). In Fig. 2, the dash-dotted line shows that the ground state of ^{8}He has large overlaps with the THSR wave function with large σ values, and the overlap has a peak structure there (∼60% around $\sigma = 3$ fm). If the ground state is mainly described by the shell-model-like wave functions, the overlap is large around the zero limit of the σ value. Also, the overlap must rapidly decrease with increasing σ value, because the THSR wave functions with large σ values are significantly different from the wave functions of the shell-model-like states. The calculated result shows that the ground state of ^{8}He is not the simple shell-model picture and the dineutron-like component is also important. However, in the case of ^{8}He, we can also see non-negligible squared overlap at small σ values (∼40% around $\sigma = 1$ fm). This is due to the admixture of shell-model-like components: the THSR wave function with zero σ value corresponds to the lowest representation of the Elliott SU(3) state. This situation is quite different in ^{7}H. In the case of ^{7}H, the squared overlap at $\sigma = 1$ fm is only 6%. Because the t-n(t-$2n$) interaction is much weaker than the ^{4}He-n (^{4}He-$2n$) interaction because of the lack of one proton in the core nucleus, the dineutron clusters are more spatially

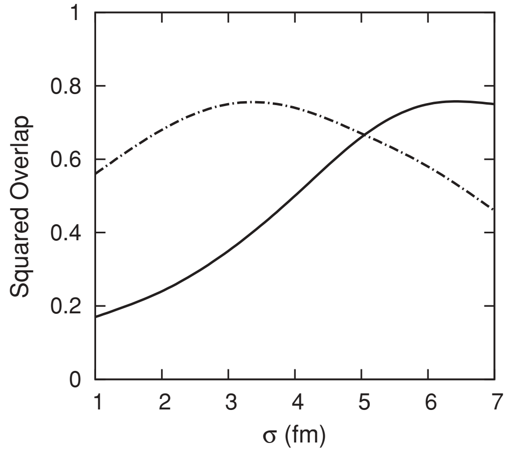

FIG. 3. The squared overlap between the obtained ground state and the THSR wave function. The solid line corresponds to the squared overlap for ^{5}H ($M = 0.56$, $B = H = 0.07$, $b = 1.60$ fm). The dash-dotted line corresponds to ^{6}He, where the wave function is the same one as in Ref. [16]. The horizontal axis represents σ.

extended in ^{7}H than in ^{8}He, which appears as the shift of the peak position (at 3 fm in ^{8}He and at 6 fm in ^{7}H). The large overlap value at the peak position suggests a well-developed dineutron cluster rather than a shell-model-like structure in ^{7}H.

Furthermore, for ^{7}H, we calculate the overlap with stronger attractive interaction ($M = 0.5$, $B = H = 0.07$, $b = 1.67$ fm). The calculated energy is 3.3 MeV from the threshold. The shape of the obtained squared overlap (dashed line in Fig. 2) is not so much different from the $M = 0.56$ case even with such a strong interaction, although it approaches the line of the ^{8}He result a bit as expected. Therefore, we can conclude that the major component of the ^{7}H wave function is described by a simple THSR wave function with large σ value ($\sim$70% at $\sigma = 6$ fm) rather than by a shell-model-like wave function ($\sim$10% at $\sigma = 1$ fm).

Although there is only one dineutron and they are not the dineutron condensate, it is instructive to show the similar values for ^{5}H and ^{6}He. In Fig. 3, the squared overlap between the obtained ground states and the THSR wave functions are shown. The solid line corresponds to the squared overlap for ^{5}H ($M = 0.56$, $B = H = 0.07$, $b = 1.60$ fm), and the dash-dotted line corresponds to the squared overlap for ^{6}He ($M = 0.60$, $B = H = 0.125$, $b = 1.46$ fm), where the wave function is the same as the one in Ref. [16] ($S_{2n} = 1.09$ MeV, $R_{\rm r.m.s.} = 2.35$ fm), which almost reproduces the experimental values ($S_{2n} = 0.98$ MeV [27], $R_{\rm r.m.s.} = 2.48$ fm [28] and 2.33 fm [29]).

For ^{5}H, the overlap reaches 75% at larger σ region ($\sigma \sim 6$ fm). We can interpret that the ground state of ^{5}H has well-developed dineutron clusters, where the main component is described by a simple wave function (the THSR-type wave function). By adding one proton to the triton core, the interaction between the core and dineutron becomes much larger. Even in such a case, the ground state of ^{6}He has the components of the THSR-type wave function with large σ values by 75%. However in the case of ^{6}He, the squared overlap with small σ value is also large (56% at $\sigma = 1$ fm). Therefore, the wave function of ^{6}He has aspects of both the shell-model-like and the dineutron-like structure.

We have investigated the dineutron correlations in ^{7}H. The ground state of ^{7}H has been solved by using the AMD triple-S with various $t + n + n + n + n$ configurations. The mixing of dineutron cluster components has been estimated by calculating the squared overlap with the THSR wave function. The calculated results show significant mixing of dineutron ($t + {}^2n + {}^2n$) components, and the dineutron clusters have a spatially extended distribution (the peak is $\sim$6 fm) much lareger than that of ^{8}He ($\sim$3 fm), where the core nucleus is changed from the polarized t cluster to ^{4}He.

This work is promoted by Bilateral Joint Research Projects of the JSPS (Japan) and the FNRS (Belgium). This work is also supported by a Grand-in-Aid for Scientific Research (17740137) from the Ministry of Education, Science and Culture and by the JSPS core-to-core program. The authors acknowledge valuable discussions with P. Schuck and Y. Kanada-En'yo at Yukawa Institute for Theoretical Physics.

[1] M. Caamaño *et al.*, Phys. Rev. Lett. **99**, 062502 (2007).
[2] M. Caamaño *et al.*, Phys. Rev. C **78**, 044001 (2008).
[3] A. A. Korsheninnikov *et al.*, Phys. Rev. Lett. **90**, 082501 (2003).
[4] H. Esbensen and G. F. Bertsch, Nucl. Phys. **A542**, 310 (1992).
[5] M. V. Zhukov, B. V. Danilin, D. V. Fadorov, J. M. Bang, I. J. Thompson, and J. S. Vaagen, Phys. Rep. **231**, 151 (1993).
[6] D. V. Fedorov, A. S. Jensen, and K. Riisager, Phys. Lett. **B312**, 1 (1993).
[7] S. Aoyama, S. Mukai, K. Kato, and K. Ikeda, Prog. Theor. Phys. **93**, 99 (1995).
[8] M. Matsuo, Phys. Rev. C **73**, 044309 (2006).
[9] K. Hagino, H. Sagawa, J. Carbonell, and P. Schuck, Phys. Rev. Lett. **99**, 022506 (2007).
[10] A. Tohsaki, H. Horiuchi, P. Schuck, and G. Röpke, Phys. Rev. Lett. **87**, 192501 (2001).
[11] Y. Funaki, A. Tohsaki, H. Horiuchi, P. Schuck, and G. Röpke, Phys. Rev. C **67**, 051306(R) (2003).
[12] N. Itagaki, M. Ito, K. Arai, S. Aoyama, and Tz. Kokalova, Phys. Rev. C **78**, 017306 (2008).
[13] Y. Kanada-En'yo, Phys. Rev. C **76**, 044323 (2007).
[14] S. Aoyama and N. Itagaki, Nucl. Phys. **A738**, 362 (2004).
[15] N. K. Timofeyuk, Phys. Rev. C **65**, 064306 (2002); **69**, 034336 (2004).
[16] S. Aoyama, N. Itagaki, and M. Oi, Phys. Rev. C **74**, 017307 (2006).
[17] N. Itagaki, A. Kobayakawa, and S. Aoyama, Phys. Rev. C **68**, 054302 (2003).
[18] V. I. Kukulin and V. M. Krasnopl'sky, J. Phys. G **3**, 795 (1977).
[19] K. Varga, Y. Suzuki, and R. G. Lovas, Nucl. Phys. **A571**, 447 (1994).

[20] P. Schuck, Y. Funaki, H. Horiuchi, G. Röpke, A. Tohsaki, and T. Yamada, Nucl. Phys. **A738**, 94 (2004).
[21] N. Itagaki, M. Kimura, C. Kurokawa, M. Ito, and W. von Oertzen, Phys. Rev. C **75**, 037303 (2007).
[22] A. B. Volkov, Nucl. Phys. **74**, 33 (1965).
[23] A. A. Korsheninnikov *et al.*, Phys. Rev. Lett. **87**, 092501 (2001).
[24] R. Tamagaki, Prog. Theor. Phys. **39**, 91 (1968).
[25] S. Okabe and Y. Abe, Prog. Theor. Phys. **61**, 1049 (1979).
[26] K. Hagino, N. Takahashi, and H. Sagawa, Phys. Rev. C **77**, 054317 (2008).
[27] F. Ajzenberg-Selove, Nucl. Phys. **A490**, 1 (1988).
[28] I. Tanihata *et al.*, Phys. Lett. **B160**, 380 (1985).
[29] L. V. Chalkov *et al.*, Europhys. Lett. **8**, 245 (1988).